Hemoglobin Control of Cell Survival/Death Decision Regulates in Vitro Plant Embryogenesis[1][W][OPEN]

Shuanglong Huang, Robert D. Hill*, Owen S.D. Wally, Giuseppe Dionisio, Belay T. Ayele, Sravan Kumar Jami, and Claudio Stasolla

Department of Plant Science, University of Manitoba, Winnipeg, Manitoba, Canada R3T 2N2 (S.H., R.D.H., O.S.D.W., B.T.A., S.K.J., C.S.); and Department of Molecular Biology and Genetics, Faculty of Science and Technology, Aarhus University-Flakkebjerg, 4200 Slagelse, Denmark (G.D.)

Programmed cell death (PCD) in multicellular organisms is a vital process in growth, development, and stress responses that contributes to the formation of tissues and organs. Although numerous studies have defined the molecular participants in apoptotic and PCD cascades, successful identification of early master regulators that target specific cells to live or die is limited. Using *Zea mays* somatic embryogenesis as a model system, we report that the expressions of two plant hemoglobin (Hb) genes (*ZmHb1* and *ZmHb2*) regulate the cell survival/death decision that influences somatic embryogenesis through their cell-specific localization patterns. Suppression of either of the two *ZmHb*s is sufficient to induce PCD through a pathway initiated by elevated NO and Zn^{2+} levels and mediated by production of reactive oxygen species. The effect of the death program on the fate of the developing embryos is dependent on the localization patterns of the two *ZmHb*s. During somatic embryogenesis, *ZmHb2* transcripts are restricted to a few cells anchoring the embryos to the subtending embryogenic tissue, whereas *ZmHb1* transcripts extend to several embryonic domains. Suppression of *ZmHb2* induces PCD in the anchoring cells, allowing the embryos to develop further, whereas suppression of *ZmHb1* results in massive PCD, leading to abortion. We conclude that regulation of the expression of these *ZmHb*s has the capability to determine the developmental fate of the embryogenic tissue during somatic embryogenesis through their effect on PCD. This unique regulation might have implications for development and differentiation in other species.

Selective elimination of overproduced, superfluous, or damaged cells by programmed cell death (PCD) is a common feature of cellular homeostasis. In conjunction with cell division and differentiation, spatial and temporal execution of the death program helps develop the organism's shape and sculpts its final form. Necrosis, autophagy, and apoptosis are the recognized forms of PCD in vertebrates (for review, see Portt et al., 2011), whereas necrosis and autophagy are the identifiable forms of PCD in plants (for review, see van Doorn et al., 2011). Common features of PCD are loss of osmoregulation in the cell, activation of caspases, nuclear and DNA fragmentation, generation of lysosomal enzymes, and mitochondrial swelling with the release of cytochrome C (for review, see van Doorn et al., 2011). Autophagy differs between vertebrates and plants in that autophagosomes are produced in the former, whereas lytic vacuoles are a common feature in plant cells undergoing PCD. Variations and flexibility in the execution of these events and presence of cross talk among the different death pathways (Whelan et al., 2010) attest to the complexity of the death program. This complexity is further aggravated by the ambiguous involvement of several signal molecules, including Zn^{2+}, in the cell death/survival decision. The participation of Zn^{2+} in cell death is dichotomous because proapoptotic and antiapoptotic effects have been shown in different systems. Although Zn^{2+} deficiencies are associated with apoptosis in some systems, including human Burkitt lymphoma B cells (Truong-Tran et al., 2000), elevated Zn^{2+} levels induce caspase activity in others (Schrantz et al., 2001; Helmersson et al., 2008).

As with vertebrates, plant PCD is an integral component of growth and development, which shapes organs through selective and controlled elimination of cells. Execution of PCD has been reported during different phases of the plant life cycle. It establishes polarity in immature embryos, it eliminates suspensor cells in mature embryos, it contributes to the formation of vascular tissue throughout development, and it is involved in senescence-related processes (Reape et al., 2008). Execution of the death pathway is also a key component of abiotic (aerenchyma formation during hypoxia; Evans, 2003) and incompatible pathogen infection (Pennell and Lamb, 1997). Although a great deal is now known about the molecular and biochemical events regulating the death pathways in vertebrates and plants, information on the mechanisms by which specific cells are targeted to either live or die is scarce.

[1] This work was supported by the National Sciences and Engineering Research Council (to R.D.H. and C.S.) and the University of Manitoba (Graduate Fellowship to S.H.).

* Address correspondence to rob_hill@umanitoba.ca.

The author responsible for distribution of materials integral to the findings presented in this article in accordance with the policy described in the Instructions for Authors (www.plantphysiol.org) is: Robert D. Hill (rob_hill@umanitoba.ca).

[W] The online version of this article contains Web-only data.

[OPEN] Articles can be viewed online without a subscription.

www.plantphysiol.org/cgi/doi/10.1104/pp.114.239335

Hemoglobins (Hbs) are ubiquitous heme-containing proteins found in all nucleated organisms (for review, see Weber and Vinogradov, 2001). Depending on organisms and tissues, they may act as oxygen carriers or stores or bind other small ligands, such as CO_2, CO, or NO. Plant Hbs have been cataloged into symbiotic (leghemoglobins) and nonsymbiotic. Leghemoglobins are generally restricted to root nodules of nitrogen-fixing plants, whereas nonsymbiotic Hbs are found in shoots and roots of both monocots and dicots (Hill, 2012). From a phylogenic perspective, Hbs are categorized into three classes (classes 1–3; Hunt et al., 2001). Classes 1 and 2 Hbs share a three-on-three α-helical loop structure surrounding the heme moiety, whereas class 3 Hbs possess a two-on-two α-helical structure, similar to truncated bacterial globins. NO scavenging is one of the major functions of plant Hbs, and evidence of their action in this fashion has been shown in plant development and in response to both biotic and abiotic stress (for review, see Hill, 2012).

Although expressed during embryo development (Smagghe et al., 2007), the majority of information related to the function of plant Hbs has been obtained during postembryonic growth. Embedded in the maternal tissue and difficult to dissect, plant embryos are not readily amenable to physiological and molecular studies. An alternative model to in vivo embryogenesis is somatic embryogenesis, the production of embryos from somatic cells. Other than elucidating key molecular mechanisms governing embryogenesis (Thorpe and Stasolla, 2001), this system has been used to show the requirement of PCD for proper embryo development. In spruce (*Picea abies*), the activation of PCD is an obligatory step for the formation of somatic embryos, and experimental suppression of the death program compromises embryogenesis (for review, see Bozhkov et al., 2005).

Using maize (*Zea mays*) somatic embryogenesis as a model system, the relationship between the expression of two maize Hbs (*ZmHb1* and *ZmHb2)*, NO, and PCD has been examined during the formation of somatic embryos. The two *ZmHb*s are shown to regulate the death program through similar mechanisms that interfere with the cascade of events mediated by NO and Zn^{2+}, the mitogen-activated protein kinase (MAPK) cascade, and accumulation of reactive oxygen species (ROS) that lead to PCD. This regulation, which influences the embryogenic pathway in a fashion consistent with the localization patterns of *ZmHb1* and *ZmHb2*, identifies Hbs as unique key regulators of the survival/death decision.

RESULTS

Suppression of *ZmHb*s Affects Somatic Embryogenesis

In maize, production of in vitro embryos through somatic embryogenesis is achieved through three distinct culture steps (Garrocho-Villegas et al., 2012; Fig. 1A). Embryogenic tissue grown on solid maintenance medium was transferred in a liquid auxin-containing proliferation (P) medium of similar composition. Cells in the P medium proliferated rapidly, and immature somatic embryos attached to the subtending embryogenic tissue became visible. After 7 d, the tissue was transferred onto a solid auxin-free development (D) medium, which allowed the immature embryos to grow into fully functional mature embryos able to germinate and regenerate viable plants. Pharmacological treatments were applied during 7 d in P medium (Fig. 1A). For the purpose of this study, immature embryos were harvested from P medium at d 7, whereas mature embryos were collected from the D medium at d 21 (Fig. 1A).

Expression and localization of two maize *Hb* genes, *ZmHb1* (AF236080) and *ZmHb2* (DQ171946; Smagghe et al., 2009; Supplemental Fig. S1), were examined during different phases of the embryogenic process. The expression of both genes gradually increased in the P medium, with a sharp increase occurring between d 1 and 7 in the D medium (Fig. 1B). To verify whether this increase was because of the removal of auxin in the D medium or other differences in chemical composition between the P and D media, the expression of the *ZmHb* genes was also measured in a D medium devoid of (−) or enriched with (+) auxin. The transcript levels of both *ZmHb1* and *ZmHb2* increased in the D medium devoid of auxin (Supplemental Fig. S2).

In immature embryos (d 7 in P medium; Fig. 1A), a different localization pattern was observed for the two *ZmHb*s (Fig. 1C). Unlike *ZmHb2*, with expression that was restricted to a cluster of basal cells anchoring the embryos to the subtending embryogenic tissue (Fig. 1C, 2 and 5) or other immature embryos (Fig. 1C, 3), *ZmHb1* transcripts were detected in extended domains of the embryos (Fig. 1C, 1 and 4).

The functional role of *ZmHb1* and *ZmHb2* in the embryogenic process was further analyzed through antisense-mediated suppression studies. Competence to produce mature somatic embryos (d 21 on D medium; Fig. 1A) was highly repressed in lines down-regulating *ZmHb1* [*ZmHb1(A)* lines] and induced in lines down-regulating *ZmHb2* [*ZmHb2(A)* lines; Fig. 1D]. These embryogenic differences were solely ascribed to a repression of the respective *ZmHb* gene, because the antisense suppression of one *ZmHb* gene did not significantly alter the expression of the other (charts in Fig. 1D). Additional studies were performed using the 368-2 *ZmHb1(A)* line and the 371-5 *ZmHb2(A)* line, because they showed the greatest differences in embryo number and the most pronounced repression of the respective *ZmHb*.

*ZmHb*s Regulate Intracellular Zn^{2+} through the NO-Dependent Metal Release from Metallothioneins

The documented ability of Hbs to scavenge NO (Weber and Vinogradov, 2001) was retained by *ZmHb1* and *ZmHb2* as revealed by the fluorescent signal of 4,5-diaminofluorescein diacetate (DAF-2DA), which is routinely used to detect cellular NO (Hebelstrup and

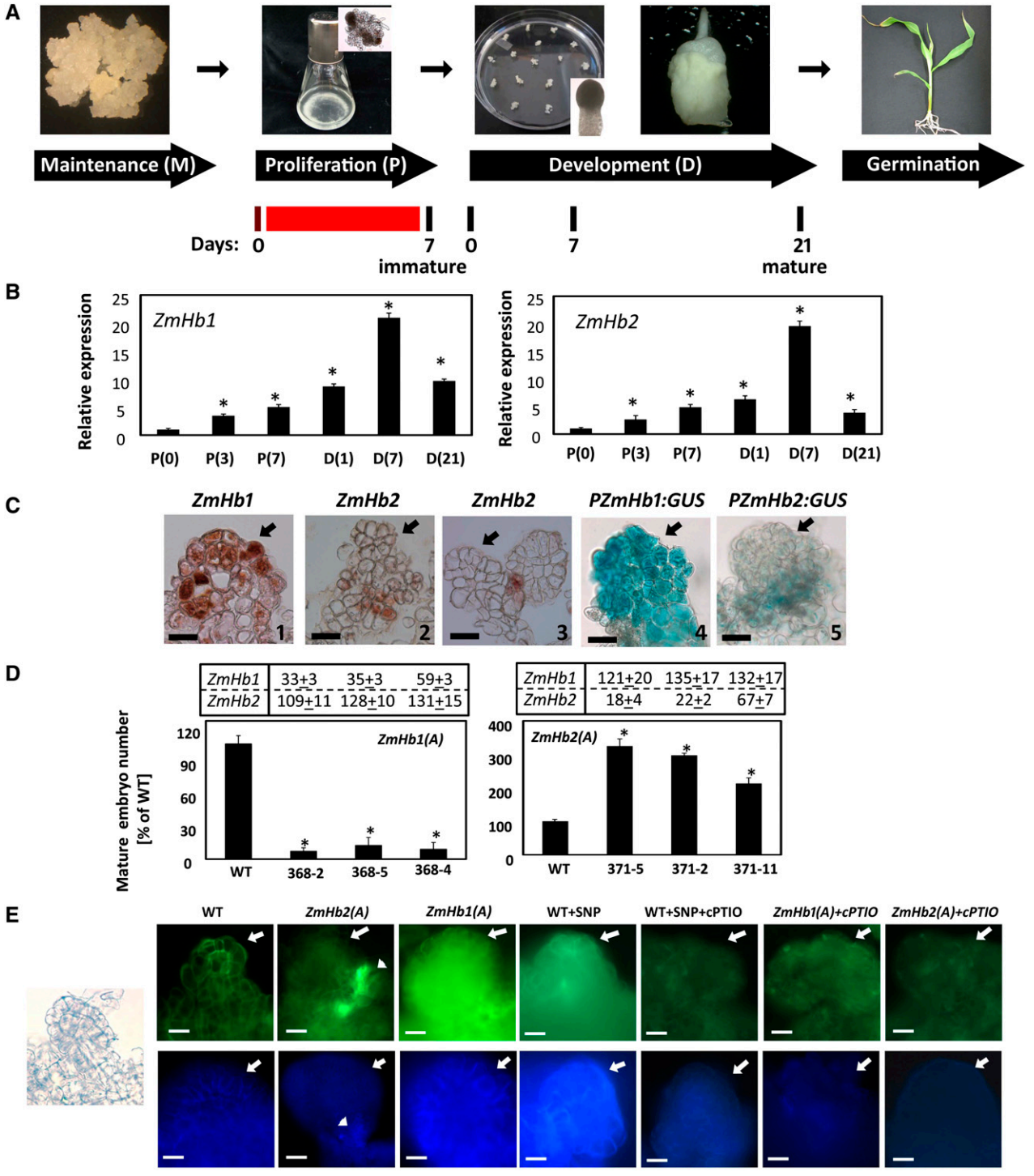

Figure 1. Hb regulation of maize somatic embryogenesis. A, Schematic representation of the maize somatic embryogenic system comprising maintenance (M), P, D, and germination (G) phases. Representative stages of embryo development and days in culture are also depicted. The red line indicates the timing of pharmacological treatments, which were all applied between d 0 and 7 in P medium. B, Expression level by quantitative RT-PCR of *ZmHb1* and *ZmHb2* during the P and D phases of embryogenesis. Values are means ± SES of three independent biological replicates and normalized to the value of P(0) set at 1. Numbers in parentheses represent days in the respective phase. *, Statistically significant difference ($P \leq 0.05$) from P(0). C, Localization of *ZmHb1* (1 and 4) and *ZmHb2* (2, 3, and 5) in immature embryos (d 7, P medium) using RNA in situ hybridization (1–3) and *PZmHb1:GUS* and *PZmHb2:GUS* reporter lines (4 and 5). Arrows indicate the apical domain of the developing embryos. Bars = 20 μm. D, Percentage of mature (d 21, D medium) somatic embryos obtained from antisense lines suppressing *ZmHb1* [*ZmHb1(A)*] or *ZmHb2* [*ZmHb2(A)*]. Values (wild type set at 100%) are means ± SES of four independent

Table I. *Effects of the NO donor DEA/NO on the release of Zn^{2+} from the recombinant MBP5 and the MBP5-ZmMT4 fusion protein*

Medium was supplemented with 0.4 mM $ZnSO_4$. Values are means ± SES of three biological replicates. Zn^{2+} measurements were performed by the dithizone method (Paradkar and Williams, 1994).

Protein	Concentration	Zn^{2+} Released		Acidification	DEA/NO
		Acidification	DEA/NO		
		mM		%	
MBP5	4.15 ± 0.13	0.01 ± 0.01	0.01 ± 0.01		
MBP5-ZmMT4	4.15 ± 0.21	0.76 ± 0.02	0.63 ± 0.05	100[a]	83[a]

[a]The percentage of Zn^{2+} recovered after the DEA/NO treatment (Zn^{2+} released by NO) compared with the acidification assay (Zn^{2+} stored in MT4).

Jensen, 2008; Elhiti et al., 2013). In the antisense lines, NO accumulation was elevated in areas where the specific *ZmHb* was detected in wild-type tissue (i.e. small clusters of basal cells in the *ZmHb2(A)* line; arrowhead in Fig. 1E, top) and a larger group of embryonic cells in the *ZmHb1(A)* line (compare Fig. 1, C with E). Specificity of the signal was verified in the wild-type line with the commonly used NO donor, sodium nitroprusside (SNP), and/or an NO scavenger, 2-(4-carboxyphenyl)-4,4,5,5-tetramethylimidazoline-1-oxyl-3-oxide (cPTIO; Hebelstrup and Jensen, 2008; Elhiti et al., 2013). Applications of cPTIO reduced NO and Zn^{2+} signals in the transformed lines.

In vertebrates, Zn^{2+} homeostasis regulates several cell responses, some of which are modulated by NO (Lee and Koh, 2010). Intracellular Zn^{2+} was detected using the membrane-permeable Zinquin-ethyl-ester (Zalewski et al., 1993), which is highly sensitive to variations in Zn^{2+} in maize embryos (Supplemental Fig. S3). Zinquin is often used to image free Zn^{2+} for its strong specificity because it does not react with other divalent cations (Helmersson et al., 2008). An increased intracellular Zn^{2+} pool was observed in cells accumulating NO, whereas cells with reduced NO content had less intense Zn^{2+} signal (Fig. 1E, bottom). The relationship between Zn^{2+} levels and NO presence was substantiated by pharmacological manipulations of NO content using SNP or cPTIO. Free Zn^{2+} level increased after applications of the NO donor SNP, whereas it decreased in cells treated with the NO scavenger cPTIO (Fig. 1E).

Despite the lack of information relative to the regulation of intracellular Zn^{2+} pool by NO in plants, the role of metallothioneins (MTs) in the storage and homeostasis of Zn^{2+} and other heavy metal is becoming more evident. Based on the arrangements of Cys residues, four types of plant MTs (MT1–MT4) have been identified (Cobbett and Goldsbrough, 2002). The expression and localization of MTs vary between tissues and organs. In both Arabidopsis (*Arabidopsis thaliana*) and barley (*Hordeum vulgare*), MT4 isoforms contribute to the storage and release of Zn^{2+} during embryogenesis (Hegelund et al., 2012; Ren et al., 2012). To investigate whether the maize ZmMT4 is capable of storing Zn^{2+} and releasing it in a high-NO environment, a recombinant maltose binding protein (MBP) fusion with ZmMT4 was constructed and expressed in *Escherichia coli*. In vivo *E. coli* feeding with $ZnSO_4$ yielded a recombinant ZmMT4 protein loaded with Zn^{2+} (Table I), which was assessed by acid release and dithizone (DTZ) measurement. Treatments with the NO donor diethylamine NONOate (DEA/NO) released a substantial percentage of the Zn^{2+} contained in the recombinant ZmMT4 during the 45-min incubation time (Table I). No Zn^{2+} was detected on DEA/NO treatment of MBP alone. The amount of Zn^{2+} released was dependent on the amount of NO provided (Supplemental Fig. S4). This unloading of Zn^{2+} clearly shows that NO can regulate intracellular Zn^{2+} level through its release from MTs, a process that has not been described in plants.

To further investigate the requirement of NO in modulating intracellular Zn^{2+} during the *ZmHb* response, we examined embryo production in the transformed lines cultured in a medium enriched with or depleted of NO and/or Zn^{2+} (Fig. 2). In the wild-type line, increased NO levels by SNP repressed the production of mature somatic embryos, whereas removal of NO by cPTIO had no effects (Fig. 2A). The possibility that SNP had toxic effects on embryogenesis was excluded by the combined applications of SNP and cPTIO. A similar embryogenic inhibition by SNP was also observed in the *ZmHb1(A)* and *ZmHb2(A)* lines, whereas cPTIO had opposite effects, promoting the production of mature somatic embryos in the former and repressing it in the latter (Fig. 2A).

Figure 1. (*Continued.*)
biological replicates. *, Statistically significant difference ($P \leq 0.05$) from wild type. Numbers in charts indicate the expression levels of *ZmHb1* or *ZmHb2* in the transgenic lines compared with the wild-type value set at 100%. E, Localization of NO (top) and Zn^{2+} (bottom) in immature embryos (d 7, P medium). Arrows indicate the apical domain of the embryos, whereas arrowheads indicate the preferential accumulation of NO and Zn^{2+} in a few cells located at the base of the embryos downregulating *ZmHb2*. Left, The micrograph shows the representative development of embryos used for the localization studies. Endogenous NO level was modulated by applications of SNP and/or cPTIO. WT, Wild type. Bars = 20 μm.

Alterations in Zn^{2+} using a pharmacological procedure described by Helmersson et al. (2008) also affected embryogenesis. Supplementation of Zn^{2+} was detrimental for the production of mature somatic embryos in all lines (Fig. 2B). Sequestration of Zn^{2+} by the Zn^{2+} chelator *N,N,N′,N′*-tetrakis(2-pyridylmethyl)ethylenediamine (TPEN) promoted embryogenesis in the *ZmHb1(A)* line and repressed embryo yield in the *ZmHb2(A)* line (Fig. 2B).

To assess the effects of combined alterations of NO and Zn^{2+} levels on embryogenesis, the cell lines were subjected to different treatments. The wild-type line, characterized by the lowest accumulation of NO (Fig. 1E), was used to test the effects of an experimental increase of NO in a low Zn^{2+} environment, whereas the NO-accumulating *ZmHb1(A)* line (Fig. 1E) was used to investigate the effects of a depletion of NO levels in a Zn^{2+}-enriched environment. The repressive effect of NO (SNP treatment) on wild-type embryo number was reversed by decreasing Zn^{2+} levels (SNP and TPEN treatment; Fig. 2C). Consistent with this observation, the increased production of mature embryos in the *ZmHb1(A)* line with low NO levels (cPTIO treatment) was abolished by elevating intracellular Zn^{2+} levels (cPTIO and Zn^{2+} treatment; Fig. 2C). These observations place Zn^{2+} as a downstream component of NO in the *ZmHb* response.

ZmHb Modulation of Embryogenesis Involves PCD and Production of ROS

In vertebrates, apoptosis and autophagy are influenced by essential trace elements. The role of Zn^{2+} homeostasis in both processes is ambiguous. Although Zn^{2+} deficiencies are associated with apoptosis in some systems (Truong-Tran et al., 2000; Helmersson et al., 2008), elevated Zn^{2+} levels induce caspase activity in others (Schrantz et al., 2001). Controlled cell death is essential in both vertebrates and plants because it shapes the body of the organism by eliminating specific cells

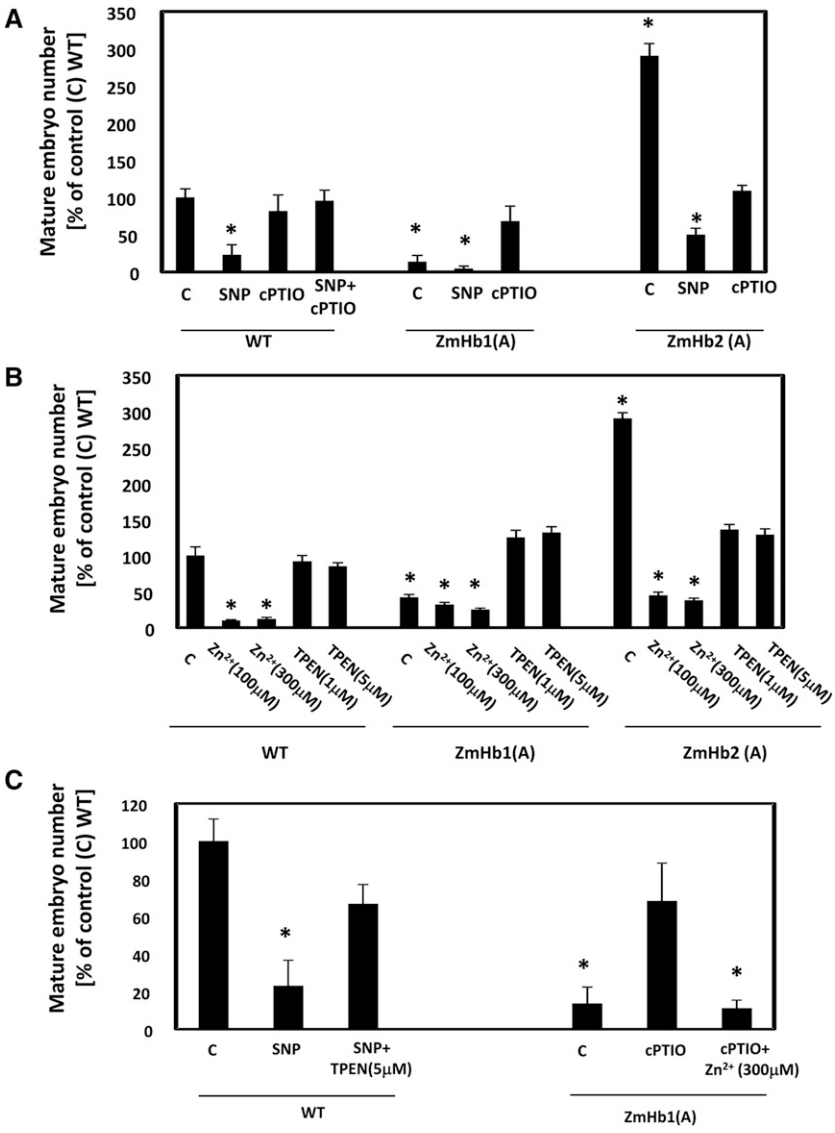

Figure 2. Effects of NO and Zn^{2+} on the production of mature somatic embryos (d 21, D medium). A, Effects of the NO donor SNP and NO scavenger cPTIO on the number of somatic embryos. B, Effects of the Zn^{2+} chelator TPEN and Zn^{2+} supplementations (using $ZnSO_4$) on the number of somatic embryos. C, Effects of combined manipulations of NO and Zn^{2+} on the number of somatic embryos. Values are means ± SEs of at least four biological replicates. *, Statistically significant differences ($P \leq 0.05$) from control (C); wild type (WT) set at 100%.

and tissues. To verify whether the *ZmHb* regulation of somatic embryogenesis is executed through PCD, we assayed nuclear DNA fragmentation using terminal deoxynucleotidyl transferase-mediated dUTP nick end labeling (TUNEL; Fig. 3A). Although no or little PCD was observed in immature wild-type embryos, the distribution of the TUNEL signals in the *ZmHb2(A)* line was restricted to small clusters of basal cells, which was in contrast to the *ZmHb1(A)* line, where PCD targeted a large number of embryonic cells (Fig. 3A). Cells undergoing PCD are most likely those suppressing *ZmHb*s and with elevated levels of NO and Zn^{2+}, which are shown by the similar distribution patterns of the TUNEL-positive nuclei, *ZmHb* expression, and NO and Zn^{2+} signals (compare Fig. 1, C and E with Fig. 3A). The requirement of NO and Zn^{2+} for the *ZmHb* regulation of PCD was confirmed pharmacologically in the wild-type line. Although increasing levels of either NO- (by SNP) or Zn^{2+}-induced PCD, depletion of NO (by cPTIO) or Zn^{2+} (by TPEN) reduced the frequency of TUNEL-positive cells (Fig. 3A). Using the *ZmHb1(A)* line characterized by the highest levels of NO and Zn^{2+} (Fig. 1E), it is shown that a reduction of NO (by cPTIO) or Zn^{2+} (by TPEN) was sufficient to reduce PCD (Fig. 3A). These results were also verified by calculating the percentage of TUNEL-positive cells (Supplemental Fig. S5).

Manifestation of PCD in plant cells is characterized by biochemical and molecular hallmarks, such as fragmentation of nuclei, increased expression of metacaspases, and caspase-like activities (Reape et al., 2008). Both antisense lines showed signs of fragmentations in the nuclei undergoing PCD and increasing caspase 3-like activity (Supplemental Fig. S6). The expression of the metacaspase *ZmMCII-3* increased significantly in the *ZmHb1(A)* line but only slightly in the *ZmHb2(A)* line. In the transgenic lines, the *ZmMCII-3* transcripts localized in similar areas, where the respective *ZmHb* was detected in wild-type tissue (compare Fig. 1C with Supplemental Fig. S6). These results suggest that expression of *ZmMCII-3* and caspase 3-like activity might be involved in the *ZmHb* mediation of PCD.

Additionally, cells programmed to die accumulate ROS (Van Breusegem and Dat, 2006). To examine whether maize cells targeted by PCD accumulated ROS, we stained with nitroblue tetrazolium and 3,3′-diaminobenzidine, which detect superoxide and hydrogen peroxide, respectively (Thordal-Christensen et al., 1997; Lin et al., 2009b). Although the specificity of each individual dye should be interpreted with due caution, the use of both ensures an accurate localization of ROS in plant cells (Lin et al., 2009b). The staining signal of superoxide and hydrogen peroxide coincided with the distribution pattern of TUNEL-positive nuclei (compare Fig. 3A with Fig. 3B), thus suggesting that ROS accumulate in cells targeted to die by the suppression of *ZmHb*s. As observed for PCD, accumulation of ROS required NO and Zn^{2+}, whereas a chelation of Zn^{2+} by TPEN decreased ROS levels in an environment enriched with NO (by SNP). These results suggest that Zn^{2+} is a necessary downstream component in the NO production of ROS (Fig. 3B).

ROS Accumulation in Maize Cells Is Required for the Execution of PCD

In plant cells, ROS homeostasis is regulated by antioxidant molecules, including reduced ascorbic acid (ASC). Through the ascorbate-glutathione redox system, ROS are scavenged in a series of sequential reactions converting ASC to dehydroascorbate (Potters et al., 2002). Depletion of cellular ASC occurs in cells overproducing ROS (Potters et al., 2002), a characteristic also observed in our system (Supplemental Fig. S7). The antioxidant properties of ASC were used to further investigate the requirement of ROS for the activation of the death program (Fig. 3C). Using the *ZmHb1(A)* line, which accumulated higher levels of NO and ROS and displayed extensive PCD (Figs. 1E and 3, A and B), it is shown that ASC reduced both NO and ROS signals as well as decreased the number of TUNEL-positive nuclei (Fig. 3C). Furthermore, exogenous ASC applications modulated embryogenesis by increasing the production of mature somatic embryos in the *ZmHb1(A)* line and decreasing it in the *ZmHb2 (A)* line to wild-type values (Fig. 3C). This finding was consistent with the opposite effects of the *ZmHb*-induced PCD on embryogenesis.

Collectively, these data suggest that suppression of the two *ZmHb*s triggers identical molecular responses, but their different localization pattern results in opposite embryogenic behavior. Repression of *ZmHb2*, which is normally expressed in the basal cells anchoring the immature embryos to the embryogenic mass (Fig. 1C), elevates NO levels, which, in turn, increase free intracellular Zn^{2+} (Fig. 1E). A rise in the Zn^{2+} pool triggers ROS-mediated PCD (Fig. 3), eliminating these anchor cells and allowing the embryos to develop further at a higher frequency (Fig. 1D). Induction of PCD through similar events also occurs in *ZmHb1* down-regulating cells. However, the enlarged localization pattern of *ZmHb1*, encompassing most of the embryo proper (Fig. 1C), results in the elimination of numerous cells (Fig. 3A), leading to embryo lethality and suppression of embryogenesis (Fig. 1D).

The Oxidative Burst Contributes to ROS Production

In plants, the ROS-generating oxidative burst is mainly controlled by NADPH oxidases, a family of membrane-bound enzymes activated in a variety of stress and developmental responses (Sagi and Fluhr, 2006). In mammalian systems, NADPH oxidase is a large protein complex comprising cytosolic regulatory proteins, which include the $p47^{phox}$ and a membrane-bound NADPH-binding cytochrome consisting of the glycosylated transmembrane protein $gp91^{phox}$ and the nonglycosylated $p22^{phox}$ (Torres and Dangl, 2005). Investigations on the function of NADPH oxidases have been limited by the reduced specificity of pharmacological inhibitors, such as 4-(2-aminoethyl)-benzenesulfonyl fluoride (AEBSF; Bayraktutan, 2005) and diphenylene iodonium (DPI; Bindschedler et al., 2006). Although effective in preventing

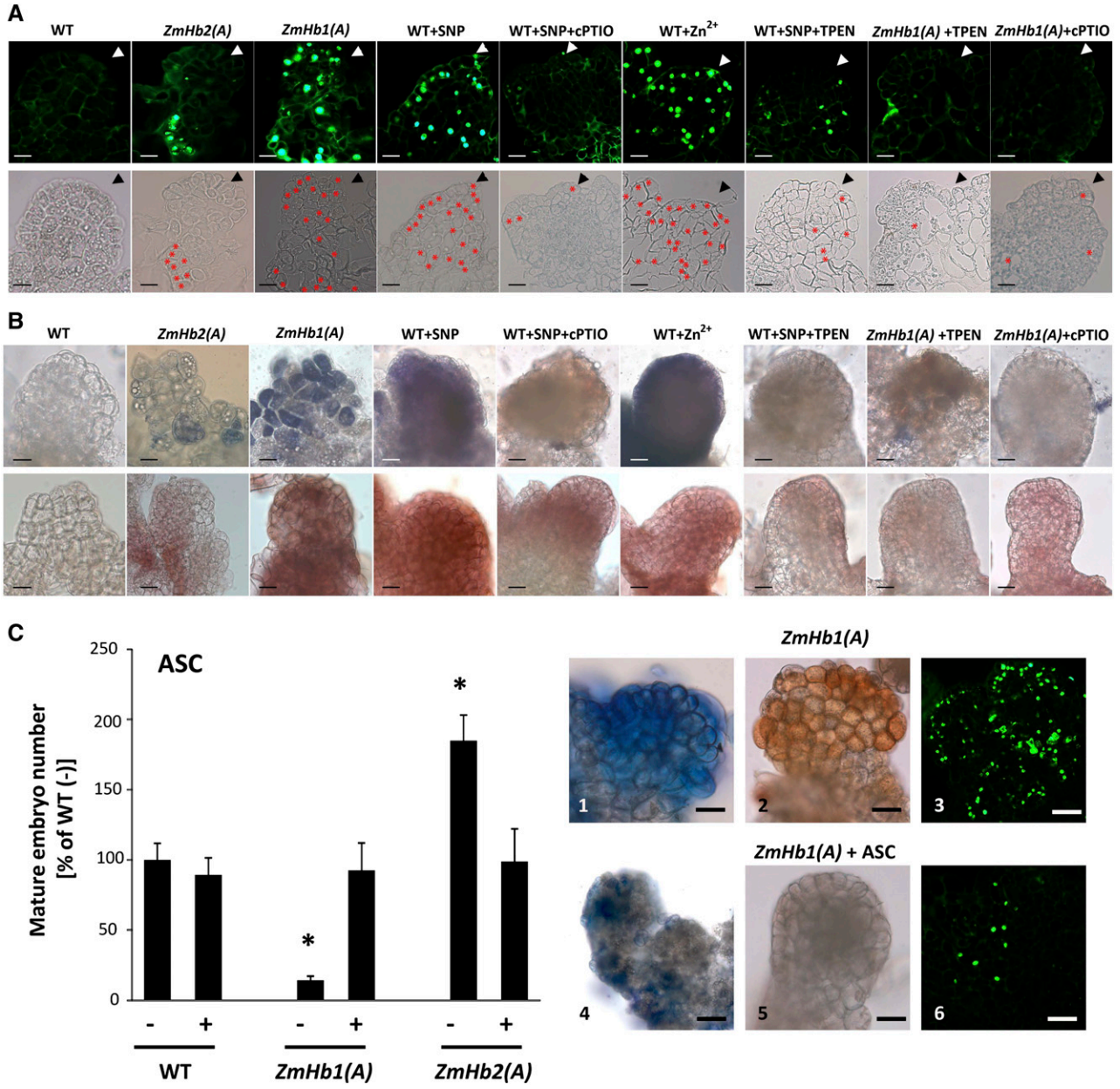

Figure 3. PCD during maize somatic embryogenesis. A, Identification of TUNEL-positive cells in immature embryos (d 7, P medium) of the *ZmHb1(A)* and *ZmHb2(A)* lines as well as embryos subjected to alterations in NO and Zn^{2+} levels using compounds from Figure 2. *, Enhanced visualization of TUNEL-positive cells in the same embryos (bottom). Arrowheads mark the apical domains of the embryos. Bars = 20 μm. B, Localization of superoxide (top) and hydrogen peroxide (bottom) in immature embryos (d 7, P medium) subjected to alterations in NO and/or Zn^{2+} level. Bars = 20 μm. C, Effects of applications of ASC on mature somatic embryo number (d 21, D medium), accumulation of superoxide (1 and 4) and hydrogen peroxide (2 and 5), and distribution of TUNEL-positive cells (3 and 6) in immature embryos (d 7, P medium). Values of embryo numbers are means ± SES of at least four biological replicates. *, Statistically significant differences ($P \leq 0.05$) from control; wild type (WT) set at 100%. Bars = 20 μm.

the activation of the ROS-producing NADPH oxidase in cell-free systems and intact stimulated macrophages by interfering with the translocation of $p47^{phox}$ to the plasma membrane (Diatchuk et al., 1997), AEBSF is a Ser protease inhibitor (Wind et al., 2010). Undesirable side effects have also been reported for DPI, which other than inhibiting NADPH oxidase in many systems (Bindschedler et al., 2006; Davies et al., 2006), also inhibits other flavoenzymes (Wind et al., 2010). In light of these side effects, although the efficacy of each individual inhibitor must be interpreted with due caution, the use of both should provide a solid indication on the participation of NADPH oxidase in the production of ROS.

Applications of both AEBSF and DPI reduced the intensity of superoxide and hydrogen peroxide signal as well as the number of TUNEL-positive nuclei in the *ZmHb1(A)* line (Fig. 4) used for its elevated levels of ROS and extensive PCD (Fig. 3, A and B). Furthermore, both inhibitors modulated embryogenesis in a pattern mimicking that resulting from depletion of ROS (compare Fig. 3C with Fig. 4) and consistent with the regulation of PCD by the two *ZmHb*s (compare Fig. 3A with Fig. 4). The identical responses obtained with both inhibitors suggest that NADPH oxidase is involved in the accumulation of ROS during maize somatic embryogenesis.

To further validate this notion, the expression pattern of four maize respiratory burst oxidase (*ZmrbohA-D*) homologs to $gp91^{phox}$, a component of the mammalian NADPH oxidase complex, was measured in immature embryos. All genes, with expression patterns that correlate to the activation of NADPH oxidase (Lin et al., 2009a), were induced in lines suppressing *ZmHb1(A)* and *ZmHb2(A)* in a fashion consistent with a regulation mediated by NO and Zn^{2+} (Supplemental Fig. S8).

Collectively, these data confirm the requirement of the oxidative burst in the *ZmHb* regulation of PCD and strongly suggest the participation of NADPH oxidases in the accumulation of ROS.

The Production of ROS Necessitates an Active MAPK Cascade

The MAPK cascade transduces many stimuli, some of which are mediated by NO (Keshet and Seger, 2010), into cellular responses. This cascade, triggered by the sequential activation of the mitogen-activated protein kinase kinase (MAPKK) and the MAPKK kinase by MAPK, culminates in downstream events, including protein phosphorylation and gene expression (Keshet and Seger, 2010). The participation of the MAPK cascade in the production of ROS was investigated pharmacologically using 2-(2-amino-3-methoxyphenyl)-4H-1-benzopyran-4-one (PD098059), an effective MAPK cascade inhibitor that prevents the phosphorylation of MAPKK in animals and plants (Favata et al., 1998; Samuel and Ellis, 2002; Wang et al., 2010). Inactivation of the MAPK cascade by PD098059 abolished the accumulation of ROS and reduced PCD in the *ZmHb1(A)* line as well as modulated embryogenesis by increasing mature embryo yield in the *ZmHb1(A)* line and decreasing it in the *ZmHb2(A)* line (Fig. 5A). These results, which phenocopy closely those obtained by depleting ROS with ASC or inhibiting NADPH oxidase with AEBSF or DPI (compare Fig. 3C with Fig. 4), identify the MAPK cascade as a requirement for the production of ROS and activation of PCD.

Suppression of the MAPK cascade by PD098059 also repressed the expression of the four maize respiratory burst oxidase homologs (*ZmrbohA-D*; Fig. 5B), a result consistent with the requirement of an active MAPK cascade for the function of NADPH oxidase (Lin et al., 2009a).

Targeted PCD in *ZmHb*-Expressing Cells Phenocopies Suppression of Hbs

Evidence presented so far suggests that the opposite embryogenic response of the *ZmHb1(A)* and *ZmHb2(A)*

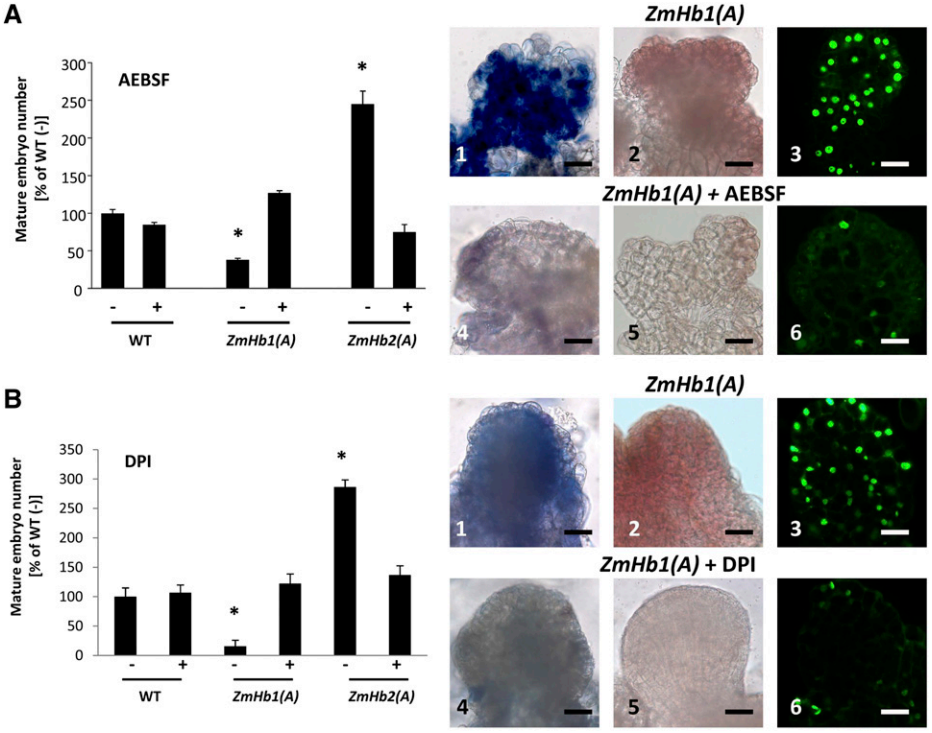

Figure 4. Requirement of NADPH oxidase in the *ZmHb* response. Effects of applications of the NADPH oxidase inhibitors AEBSF (A) and DPI (B) on mature (d 21, D medium) somatic embryo number, accumulation of superoxide (1 and 4) and hydrogen peroxide (2 and 5), and distribution of TUNEL-positive cells (3 and 6) in immature embryos (d 7, P medium). Values of embryo numbers are means ± SEs of at least four biological replicates. *, Statistically significant differences ($P \leq 0.05$) from wild type (WT; −) set at 100%. Bars = 20 μm.

lines is caused by the execution of PCD in different domains encompassing a large number of cells in the *ZmHb1(A)* embryos and a few cells anchoring the embryos to the embryogenic tissue in the *ZmHb2(A)* line. To show more precisely that cell death in these domains is a sufficient factor responsible for the observed embryogenic behavior, we induced death in *ZmHb*-expressing cells by driving the Arabidopsis gene *KISS OF DEATH* (*KOD*), a known executor of PCD (Blanvillain et al., 2011), under the control of *ZmHb1* or *ZmHb2* promoters. Expression of *AtKOD* was sufficient to induce death in *ZmHb*-expressing domains (compare Fig. 1C with Fig. 6A). Furthermore, the embryogenic response in the *PZmHb1:AtKOD* and *PZmHb2:AtKOD* lines mimicked that of the *ZmHb1(A)* and *ZmHb2(A)* lines, respectively (compare Fig. 1D with Fig. 6B), thereby showing the sufficient role of PCD in the *ZmHb* regulation of embryogenesis.

DISCUSSION

*ZmHb*s Modulate Somatic Embryogenesis through PCD

Somatic embryogenesis, the ability to generate embryos from somatic cells, has been often used as a model system to investigate basic aspects of plant growth and development because the embryogenic pathway can be easily controlled, manipulated, and/or redirected (Thorpe and Stasolla, 2001). In many plant species, including maize, an obligatory event of this process is the differentiation of immature somatic embryos from the surface of the embryogenic tissue consisting of a heterogeneous cell population. This differentiation step is facilitated by removal of plant growth regulators (Fig. 1A), and in spruce, it requires the selective elimination of embryogenic cells through PCD (Filonova et al., 2000). Abrogation of the death program using either a pharmacological approach or PCD-deficient cell lines decreases the number of somatic embryos (Bozhkov et al., 2005). The programmed nature of cell death during spruce embryogenesis was confirmed by the requirement of metacaspases, proteases with similar functions to animal caspases that are components of the late phases of the apoptotic pathway (Bozhkov et al., 2005). However, identification and characterization of molecular components participating in the early phases of the developmental PCD process, not only in embryogenesis but also during advanced stages of animal and plant development, have been elusive (Elmore, 2007).

Here, we show that the spatial regulation of *ZmHb*s is an early factor of the death program, which influences maize somatic embryogenesis. Suppression of both *ZmHb1* and *ZmHb2* triggers the death program in specific domains of the embryogenic tissue, resulting

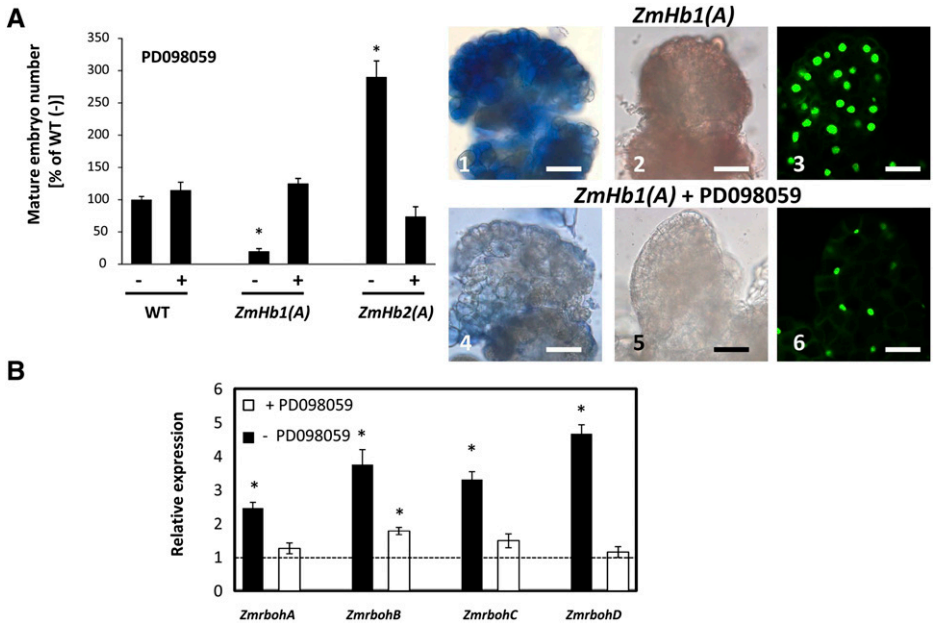

Figure 5. An active MAPKK cascade is required in the *ZmHb* response. A, Effects of applications of the MAPKK inhibitor PD098059 on mature somatic embryo (d 21, D medium) number, accumulation of superoxide (1 and 4) and hydrogen peroxide (2 and 5), and distribution of TUNEL-positive cells (3 and 6) in immature embryos (d 7, P medium). Values of embryo numbers are means ± SES of at least four biological replicates. *, Statistically significant differences ($P \leq 0.05$) from control wild type (−) set at 100%. Bars = 20 μm. B, Expression level of the four NADPH respiratory burst oxidase homologs (*ZmrbohA-D*) in the *ZmHb1(A)* tissue (d 7, P medium) cultured in the presence (+) or absence (−) of PD098059. Values are means ± SES of three independent biological replicates and normalized to the expression level of each gene in the wild-type line (set at 1). WT, Wild type. *, Statistically significant difference ($P \leq 0.05$) from wild type.

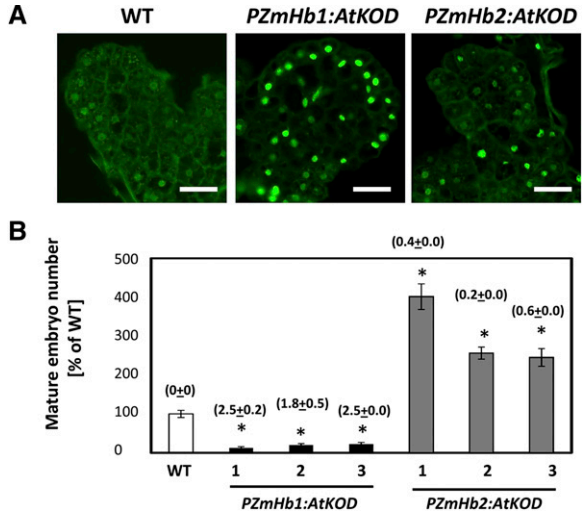

Figure 6. Induced cell death in *ZmHb*-expressing domains regulates embryogenesis. A, Identification of TUNEL-positive cells in immature embryos (d 7, P medium) obtained from the *PZmHb2:AtKOD* lines, the *PZmHb1:AtKOD* lines, and the wild-type line. Bars = 20 μm. B, Number of mature embryos (d 21, D medium) produced by three *PZmHb1:AtKOD* lines and three *PZmHb2:AtKOD* lines. Numbers in parentheses indicate the KOD-actin ratio in the respective lines. Values are means ± SEs of four biological replicates and expressed as a percentage of wild type (set at 100%). WT, Wild type. *, Statistically significant difference ($P \leq 0.05$) from wild type.

in embryogenic outcomes consistent with their respective localization patterns. Although suppression of *ZmHb1* triggers death in extended domains of embryogenic tissue, leading to embryo abortion, suppression of *ZmHb2* eliminates selected cells (i.e. the anchor cells) connecting the developing embryos to the subtending tissue and increases the formation of mature somatic embryos. Although the effects of the *ZmHb2*-mediated dismantling of anchor cells on embryo formation are beyond the scope of this work, they might be required for shaping the embryo body and promoting growth, which was documented in animal embryogenesis (Elmore, 2007) or, most likely, reducing embryonic density, an impeding factor during in vitro embryogenesis (Thorpe and Stasolla, 2001), through the physical separation of immature embryos from the embryogenic tissue.

The possibility that factors other than PCD are accountable for the embryogenic behavior of the *ZmHb*s-suppressing lines was dismissed by triggering death in *ZmHb1*- and *ZmHb2*-expressing domains using KOD. Identified as an early inducer of the death pathway in Arabidopsis, where it contributes to the depolarization of the mitochondria membrane in the Bax-mediated death pathway, heterologous expression of KOD is sufficient to activate the suicide mode (Blanvillain et al., 2011). Expression of KOD in *ZmHb*s domains closely phenocopied the death pattern and the embryogenic response of lines suppressing *ZmHb*s (compare Figs. 1D, 3A, and 6), a similarity that proves unequivocally the sufficient requirement of the death program for the observed behavior of the transformed lines. In addition to regulating the cell death/survival decision during embryogenesis, as evidenced by our results, plant Hbs might fulfill a similar function during postembryonic development in an analogous fashion to animal neuroglobins. Expressed at high levels in metabolically active cells, neuroglobins protect the brain from Alzheimer's disease by preventing neuron PCD (Khan et al., 2007; Greenberg et al., 2008) through mechanisms interfering with apoptotic events, such as the release of mitochondrial cytochrome C (Brittain et al., 2010). In plants, *Hbs* are regulated by many abiotic and biotic stress responses characterized by the manifestation of PCD (Hill, 2012). Independent studies show that overexpression of *Hbs* reduces aerenchyma formation (Dordas et al., 2003) and represses cell death after pathogen infection (Mur et al., 2012).

ZmHb Regulation of PCD Is Mediated by Cellular NO and Zn^{2+} and Requires ROS

A key role played by plant Hbs during development and stress responses is to scavenge NO through an NADH-dependent dioxygenase (Igamberdiev et al., 2014). In harmony with previous studies documenting that suppression of *AtHbs* in Arabidopsis increased cellular NO and applications of NO donors had an antagonistic effect to AtHbs (Hebelstrup and Jensen, 2008), our results showed a rise in NO in cells suppressing *ZmHb1* or *ZmHb2* (Fig. 1E). Elevated NO levels were apparent in many embryonic cells of the *ZmHb1(A)* line and a few basal embryonic cells of the *ZmHb2(A)* line. These NO-enriched domains coincided with the localization patterns of the respective *ZmHb* in the wild-type line (compare Fig. 1C with Fig. 1E). DAF-2DA fluorescence, as an indicator of NO presence, must be interpreted with caution (Mur et al., 2011). DAF-2DA fluorescence is quenched at basic pH, whereas PCD is associated with acidification of the cytoplasm (Bosch and Franklin-Tong, 2007). Fluorescence quenching caused by cellular basic pHs should not, therefore, be an issue in this circumstance, and in any event, fluorescence quenching should reduce the observed fluorescence, not increase it. Ascorbate and dehydroascorbate can also react with DAF-2DA, resulting in fluorescence similar to that observed with NO. Previous work (Igamberdiev et al., 2006) has shown that expression of Hb increases cell ascorbate and dehydroascorbate. In this work, no fluorescence was observed in cells with suppressed levels of NO. Furthermore, lower levels of reduced ASC were observed in cells of *ZmHb1(A)* and *ZmHb2(A)* lines (Supplemental Fig. S7). Increases in ascorbate/dehydroascorbate cell levels resulting in false NO detection are unlikely in this situation.

Many studies suggest that, in both animals and plants, accumulation of NO modulates several developmental and physiological responses, including PCD (Brüne, 2003). The participation of NO in the death

program is dichotomous because both antiapoptotic and proapoptotic pathways have been shown to be regulated by NO (Brüne, 2003). Proapoptotic pathways are triggered by NO through a variety of mechanisms, including the inhibition of respiration and reduction in membrane potential, the activation of caspase activity (Brüne, 2003), and the covalent modification of target proteins by nitrosylation (for review, see Igamberdiev et al., 2014). During maize embryogenesis, the increased levels of NO in *ZmHb*-suppressing cells induce PCD (Fig. 3A), and modulation of NO levels affects embryogenesis in a pattern consistent with the expression of *ZmHb*s. Specifically, a reduction of NO with cPTIO increases the number of mature somatic embryos in the *ZmHb1(A)* line, whereas it reduces it in the *ZmHb2(A)* line (Fig. 2).

Accumulation of NO elevated the levels of cellular Zn^{2+}, an important regulator of cellular integrity and response to endogenous and exogenous stimuli (Roohani et al., 2013). Elevated Zn^{2+} signals were detected in domains enriched in NO and suppressing *ZmHb*s (Fig. 1E) as well as in cells treated with the NO donor SNP (Fig. 1E). Furthermore, depletion of NO with cPTIO reduced Zn^{2+} levels. The requirement of NO for Zn^{2+} accumulation can be ascribed, at least in part, to the ability of NO to release Zn^{2+} from MTs (Table I; Supplemental Fig. S4), small heavy-metal binding proteins able to regulate cellular Zn^{2+} homeostasis (St Croix et al., 2002). The participation of MTs in NO signaling by sequestration or release of Zn^{2+} is a unique concept in plants, which other than having potential central roles in other NO-mediated responses unrelated to PCD, provide evidence of similar NO-regulatory mechanisms operating across organisms. In both hippocampus and endothelial cells, NO increases the amount of labile Zn^{2+} (Berendji et al., 1997; Cuajungco and Lees, 1998), and elevated Zn^{2+} levels can be generated from the destruction of the Zn^{2+}-sulfur clusters of MTs by NO (Aravindakumar et al., 1999). In animal cells, the contribution of the MT-mediated Zn^{2+} release to the overall cellular Zn^{2+} pool can be significant and is detectable with the same Zn^{2+}-specific fluorophore Zinquin (St Croix et al., 2002) used in this study.

Unequivocal experimental evidence indicates that elevation of Zn^{2+} levels in *ZmHb*-suppressing maize cells mediates the NO activation of PCD. First, chelation of Zn^{2+} abolishes death by NO, whereas increasing Zn^{2+} levels induce PCD in environments depleted of NO (Fig. 3). Second, manipulations of Zn^{2+} in the culture medium override the effects of NO on embryo yield (Fig. 2). The proapoptotic role of Zn^{2+} reported in our study agrees with work on animal systems (Wätjen et al., 2002; Land and Aizenman, 2005), which show that the death-triggering accumulation of Zn^{2+} originates solely from MTs (Lee et al., 2003), but not with others documenting PCD in Zn^{2+}-deficient cells (Rogers et al., 1995; Helmersson et al., 2008). This discrepancy is possibly caused by differences in perception of Zn^{2+} homeostasis operating across organisms. When manifested, the proapoptotic role of Zn^{2+} in animal cells is often mediated by ROS (Zhang et al., 2007), key regulators of developmental and environmental death programs (Elmore, 2007). This finding is in agreement with our results showing the accumulation of ROS in Zn^{2+}-supplemented cells, their depletion in Zn^{2+}-deficient cells (Fig. 3B), and the abolishment of the death program after scavenging of ROS by ASC in the *ZmHb1(A)* line characterized by high levels of Zn^{2+} (Fig. 3C). Furthermore, the observation that Zn^{2+} manipulations (supplementation or chelation) override the effects of NO on ROS production (Fig. 3B) places ROS downstream of NO and Zn^{2+} in the Hb response.

Inhibition of the Oxidative Burst and MAPK Cascade Abolishes ROS Formation

Generation of ROS in plants occurs through an oxidative burst triggered by diverse mechanisms, some of which involve NADPH oxidases, membrane-bound enzymes implicated in several responses, including PCD (Sagi and Fluhr, 2006). A reduction in ROS production during maize embryogenesis was achieved pharmacologically using both AEBSF and DPI (Diatchuk et al., 1997; Tiwari et al., 2002). Other than decreasing superoxide and hydrogen peroxide, a result consistent with previous studies (Bindschedler et al., 2006; Davies et al., 2006), these inhibitors reduced PCD in the *ZmHb1(A)* line characterized by elevated levels of ROS and TUNEL-positive nuclei (Fig. 4). Furthermore, both AEBSF and DPI abolished the effects of *ZmHb* suppression on embryogenesis, consistent with the reduction of ROS and PCD (compare Fig. 3C with Fig. 4).

Additional evidence supporting the involvement of NADPH oxidase in the accumulation of ROS during the *ZmHb*s regulation of embryogenesis is apparent by the behavior of the four *ZmrbohA-D* genes, homologs of the human neutrophil pathogen-related $gp91^{PHOX}$ (a component of the NADPH oxidase) that are expressed at high levels during active production of ROS by NADPH oxidases (Lin et al., 2009a). Suppression of *ZmHb1* or *ZmHb2* induces the expression of the four genes through the mediation of NO by Zn^{2+} (Supplemental Fig. S8).

Activation of the oxidative burst is linked to several transduction mechanisms, including the MAPK cascade (Lin et al., 2009a), which transduces many stimuli, some of which are mediated by NO (Browning et al., 2000). Inhibition of the MAPK cascade by the cell-permeable PD098059, which prevents the phosphorylation of MAPKK (Favata et al., 1998; Samuel and Ellis, 2002; Wang et al., 2010), reduces ROS production, abolishes the death program, and modulates embryogenesis in a pattern consistent with the depletion of ROS (Fig. 5A). The requirement of active MAPK for the accumulation of ROS might be exercised through the transcription of the four *ZmrbohA-D* (Fig. 5B), the expressions of which have been shown to correlate to the activation of NADPH oxidase (Lin et al., 2009a).

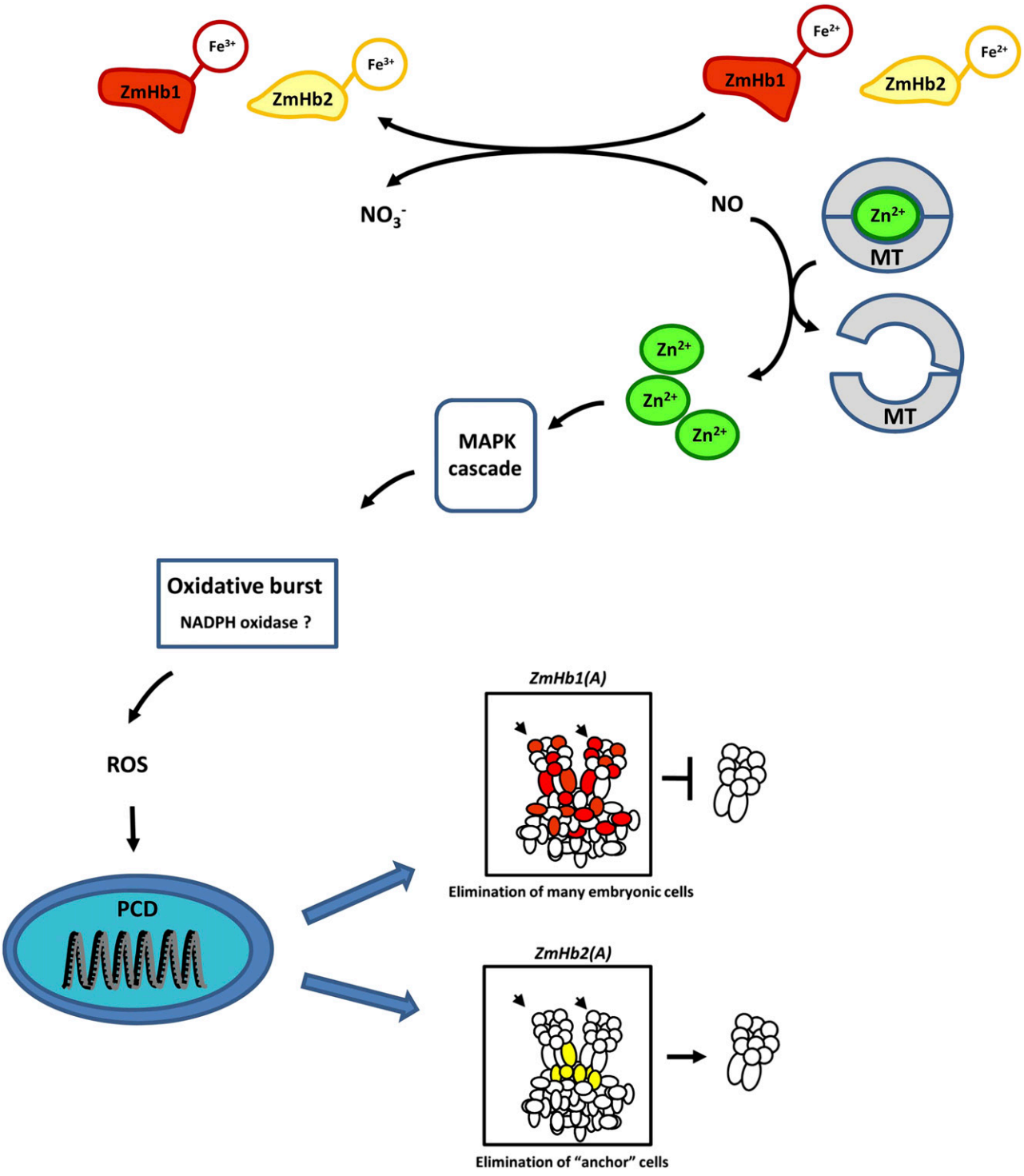

Figure 7. Proposed model of *ZmHb* action during somatic embryogenesis. Suppression of *ZmHbs* releases the inhibitory effects of NO on PCD through a cascade involving intracellular Zn^{2+}, the MAPK cascade, and accumulation of ROS, which are possibly mediated by NADPH oxidase. The distinct expression domains of *ZmHb1* and *ZmHb2* identify cells targeted by PCD and, ultimately, embryo formation. Cells undergoing PCD in the two lines [red, *ZmHb1(A)*; yellow, *ZmHb2(A)*] are outlined. Small arrows indicate the apical domain of developing embryos embedded in the embryogenic tissue.

A Unique Model Linking *ZmHb*s to Cell Death/Survival Decision during in Vitro Embyrogenesis

Results presented here fit a model in which *ZmHb* controls PCD by regulating cellular NO during maize somatic embryogenesis (Fig. 7). NO is produced as an initiator of the cascade of events ending in death of the cell. Most of the PCD pathway has been previously been described, but this work has shown the unique finding that Zn^{2+}, like in vertebrate systems, is a critical component in this cascade and released from MTs. Depending on characteristics within a specific maize embryonic cell, *ZmHb1* or *ZmHb2* may be expressed to inhibit this process. The oxygenated form of the Hb reacts with cellular NO, producing nitrate and methemoglobin (Hb [Fe^{3+}]). Therefore, the cellular expression of a specific *Hb* gene has the capability to determine the fate of that cell under conditions where mobile or transportable hormones or effectors, such as auxin, ethylene, or NO, are present in an organ. Expression of *ZmHb1* during maize somatic embryogenesis protects a large number of embryonic cells from PCD by scavenging NO; therefore, when this gene's expression is suppressed [*ZmHb1(A)*], significant embryo abortion occurs. Expression of *ZmHb2* protects a few basal embryonic cells from PCD. Suppression of expression of this gene [*ZmHb2(A)*] results in death of these anchor cells, increasing the number of mature somatic embryos produced. Programming of PCD in suspensor cells to establish embryo polarity plays a critical role in survival and development during zygotic embryogenesis (Smertenko and Bozhkov, 2014). Our results would suggest that the two maize Hbs may function to both protect the developing maize embryo from PCD (*ZmHb1*) and orchestrate the timing of suspensor PCD (*ZmHb2*) during zygotic embryogenesis.

Manifestation of PCD is also important for key events during the in vivo reproductive phase. The dismantling of the suspensor during the middle late phases of embryogenesis, the selective elimination of nucellus and aleurone cells during endosperm development, pollen-stigma interaction in the initial steps of fertilization, male and female organ sculpturing in developing flowers, and parthenogenesis are all examples of events modulated by PCD. Based on the premises of this model, it is possible that Hbs are intimately linked with these events, and their manipulation can be used as a tool to enhance the reproductive outcome.

It cannot be excluded that the regulation of PCD by Hbs can also operate across species. The majority of plants that have had Hbs identified contain at least two Hb genes, with rice (*Oryza sativa*) having as many as five genes (Vázquez-Limón et al., 2012). Cytoglobin and neuroglobin are two Hbs that potentially could function in a similar fashion in vertebrates (Burmester and Hankeln, 2009). They are up-regulated during hypoxia, capable of scavenging NO, and prevent PCD. We conclude that *ZmHb*s modulate somatic embryogenesis in maize through PCD and identify Hbs as potential regulators of morphogenesis in other systems.

MATERIALS AND METHODS

Plant Material and Treatments

Maize (*Zea mays*) Hi II Type II embryogenic tissue was obtained from the Plant Transformation Facility at Iowa State University (http://agron-www.agron.iastate.edu/ptf/). Somatic embryogenesis was induced as reported by Wang and Frame (2009) by transferring embryogenic tissue maintained on a solid 2,4-dichlorophenoxyacetic acid-containing maintenance medium into a liquid P medium of similar composition. After 7 d, the tissue was plated on solid hormone-free D medium to allow embryo maturation, which lasted 21 d. Pharmacological treatments were carried out for 7 d in the P medium. The NO donor SNP was applied at a concentration of 10 μM, and the NO scavenger cPTIO was applied at a concentration of 100 μM (Elhiti et al., 2013). $ZnSO_4$ was used as a Zn^{2+} source and applied at a concentration of 100 or 300 μM (Helmersson et al., 2008). In the Zn^{2+} supplementation experiments, control cells were also grown in a medium devoid of $ZnSO_4$. The membrane-permeable Zn^{2+} chelator TPEN was applied at a concentration of 1 or 5 μM (Helmersson et al., 2008). The specific inhibitor of MAPKK PD098059 was administered at a concentration of 50 μM (Wang et al., 2010). The NADPH oxidase inhibitors AEBSF and DPI were applied at concentrations of 1 mM and 5 μM, respectively (Diatchuk et al., 1997; Drummond et al., 2011; Ryder et al., 2013). Reduced ASC was used at a concentration of 100 μM (Stasolla and Yeung, 1999). Treatments were interrupted at d 7 in the P medium, and the tissue was either cultured on solid D medium to assess embryo yield or collected for gene expression, immunological, and histological analyses. When not specified, $ZnSO_4$ and TPEN were applied at concentrations of 300 and 5 μM, respectively.

Plant Transformation

For construction of antisense maize lines, the two Hbs, *ZmHb1* (AF236080) and *ZmHb2* (DQ171946), were amplified from complementary DNA (cDNA) prepared from maize embryogenic tissue by reverse transcription (RT)-PCR using gene-specific primers and subcloned into a pGEM-T Easy vector (Promega). Sequences were confirmed by DNA sequencing, and *Bam*HI sites were added to both 5′ and 3′ ends of both genes by PCR. The maize polyubiquitin1 (*ubi-1*) promoter was isolated from pUbiSXR vector, and *Kpn*I restriction sites were added to the 5′ and 3′ ends by PCR. The nopaline synthase terminator was isolated from pBI121 with *Sac*I restriction sites and added to the 5′ and 3′ ends. The entire cassette was assembled through sequential ligation of the *ubi-1* promoter, *nos-t*, and *ZmHb1* or *ZmHb2* into pBluescript SK−. Confirmed antisense constructs were cobombarded into immature maize embryos and selected on glufosinate-containing media (Wang and Frame, 2009).

For the promoter constructs, putative *PZmHb1* and *PZmHb2* were isolated by PCR from maize Hi II Type II callus genomic DNA using specific primers (MaizeGDB, http://www.maizegdb.org/; BDGP, http://www.fruitfly.org/; Zhao et al., 2008). The promoters (898 and 1,251 bp, respectively) were subcloned into pGEM-T Easy vector and confirmed by DNA sequencing. Using Gateway Cloning Technology (Invitrogen), both promoters were assembled into the destination vector pKGWFS7 (Karimi et al., 2002) to generate *PZmHb1:GUS* and *PZmHb2:GUS* lines.

For the KOD constructs, *AtKOD* was isolated by PCR from genomic DNA of Arabidopsis (*Arabidopsis thaliana*) ecotype Colombia-0 using gene-specific primers (Blanvillain et al., 2011), subcloned into pGEM-T Easy vector, and confirmed by DNA sequencing. The cloning fragments were amplified by *Spe*I-AtKOD-F and puc19-M13-R primers and ligated into the *Spe*I-digested and -dephosphorylated *pGEM-T:PZmHb1* and *pGEM-T:PZmHb2*, respectively. Using Gateway Cloning Technology (Invitrogen), both *PZmHb1:AtKOD* and *PZmHb2:AtKOD* were transferred into the destination vector pEarleygate 301 (Earley et al., 2006).

All primers used are listed in Supplemental Table S1.

Isolation of the Maize Embryo-Specific ZmMT4

Total RNA was isolated from wild-type maize tissue using the Dynabeads Kit (Life Technologies). The cDNA of ZmMT4 embryo-specific U10696 (protein accession no. CAA84233; Leszczyszyn et al., 2013) was obtained by RT-PCR. The amplified product was purified and cloned into the pCR4-blunt TOPO vector (Life Technologies) and confirmed by sequencing. An MBP fusion construct was assembled in pMAL-c5X vector (NEB) using an Infusion strategy (Clontech) by linearizing the vector with *Xmn*I and *Eco*RI followed by amplification with the primers MT4_fw and MT4_rev (Supplemental Table S1).

ZmMT4 Expression and Purification

A single colony of NEB expression *Escherichia coli* harboring the pMAL-c5X vector alone or the positive vector containing ZmMT4 fusion was used to inoculate an overnight starter culture in 4 mL of Luria-Bertani broth incubated at 37°C with vigorous shaking. Two milliliters of the starter was used to inoculate 200 mL of double-concentrated Luria-Bertani broth grown at 37°C. When the optical density$_{600}$ reached 4.5, the expression was induced by 0.5 mM isopropyl-β-D-1-thiogalactoside in a medium supplemented with or without 0.4 mM $ZnSO_4$. The cells were grown for an additional 3 h, harvested by centrifugation, and then resuspended in 8 mL of extraction buffer (0.1 M Tris-HCl, pH 8.0, 0.5 M NaCl, 1 mM EDTA, 1 mM AEBSF, 10 μM trans-epoxysuccinyl-L-leucylamido(4-guanidino)butane, 20 μM Bestatin, 0.1 mM Phosphoramidon, 4 mM dithiothreitol, 0.01% [v/v] Triton X-100, and 20% [v/v] glycerol). After sonication, the lysate was clarified by centrifugation and purified on 10 mL of amylose resin according to the manufacturer's specifications (NEB). Eluted control MBP and MBP-ZmMT4 fusion proteins were dialyzed and concentrated using vivaspin 20 centrifugal devices (GE Healthcare). Approximately 10 mg of recombinant MBP was recovered from 200 mL of culture. Protein quantification was performed with the method by Bradford (1976), whereas purity was confirmed by SDS-PAGE with Coomassie staining.

Release of Zn^{2+} from the Purified ZmMT4

The NO donor DEA/NO (sodium salt hydrate) was prepared as a 0.5 M stock solution in 10 mM NaOH. To quantify the presence of Zn^{2+} in the purified MBP or MBP-ZmMT4 proteins, 0.2 to 0.26 mg of each protein, in triplicate, was incubated with 1 N HCl for 45 min at room temperature and centrifuged at 20,000*g* for 2 min. The release of Zn^{2+} was quantitatively evaluated by DTZ (diphenylthiocarbazone) by following published protocols (Paradkar and Williams, 1994).

For the Zn^{2+} release by DEA/NO, 1 concentration of ZmMT4 and MBP (as negative control), in triplicate, was incubated at room temperature for 45 min in 0.05 M Tris-HCl (pH 7.5) with 3 mM DEA/NO or the same amount of water (negative control). The amount of Zn^{2+} released was directly assayed by the DTZ method described above.

The choice of different NO donors (SNP for embryogenesis and DEA/NO for the MTs experiment) was based on their different characteristics. SNP is the NO donor used most routinely in vivo (Hebelstrup and Jensen 2008; Elhiti et al., 2013). NO release from SNP is not spontaneous but relies on chemical reactions after SNP is absorbed by the cells (Miller and Megson, 2007). Therefore, SNP was used only for the embryogenesis studies but not the MTs experiment. The effectiveness of SNP was always verified by monitoring NO levels. DEA/NO spontaneously dissociates, releasing NO at neutral or slight alkaline pH. The release of NO from DEA/NO is more homogeneous and more suitable for in silico studies because it can be regulated/controlled by adjusting the pH of the buffer used. A pH of 7.5 was used for the MT experiment. Because of its pH-dependent properties, the use of DEA/NO is not recommended in vivo, especially in culture, where changes in pH often occur over time.

In Situ Localization of NO, Zn^{2+}, and PCD

NO was assayed using DAF-2DA (Elhiti et al., 2013). Zinquin-ethyl-ester was used to localize Zn^{2+} (Helmersson et al., 2008). Nuclear DNA fragmentation was detected with the In Situ Cell Death Detection Kit-Fluorescein (Roche). Tissue was fixed in 4% (w/v) paraformaldehyde, dehydrated in ethanol series, and embedded in wax. Sections (10 μm) were dewaxed in xylene and labeled with the TUNEL kit (Roche) according to the manufacturer's protocol, with the exclusion of the permeabilization step by proteinase K. Omission of terminal deoxynucleotidyl transferase was used for negative controls.

Localization of Superoxide, Hydrogen Peroxide, and Reduced ASC

Localization of hydrogen peroxide in maize cells was performed as described by Thordal-Christensen et al. (1997). Suspension cells (0.2 mL) were stained with 3,3′-diaminobenzidine (pH 3.8) for 3 h in the dark. Superoxide was visualized by incubating cells in a solution containing 0.05% (w/v) nitroblue tetrazolium, 10 mM sodium azide, and 50 mM phosphate-buffered saline (pH 7.6; Lin et al., 2009b). Reduced ASC was localized following the procedure by Liso et al. (2004).

Expression Studies

TRI Reagent Solution was used to extract RNA following the manufacturer's instruction (Invitrogen), and the High-Capacity cDNA Reverse Transcription Kit (Applied Biosystems) was used for cDNA synthesis. Gene expression studies were performed by quantitative RT-PCR. All primers used for gene expression studies are listed in Supplemental Table S1. The relative gene expression level was analyzed with the $2^{-\Delta\Delta CT}$ method (Livak and Schmittgen, 2001) using actin as the reference gene.

Expression of *AtKOD* was detected by quantitative RT-PCR, Taqman technology using AtKOD-F/R with AtKOD-FAM probe, and Actin1-F/R with Actin1-HEX probe (Supplemental Table S1).

Caspase-Like Activity

Caspase 3-like activity was assayed using the substrate Ac-DEVD-AFC (Coffeen and Wolpert, 2004; Ye et al., 2013). The assay was conducted using a fluorescence spectrophotometer (excitation of 400 nm and emission of 505 nm).

RNA in Situ Hybridization

RNA in situ hybridization studies were conducted as described (Elhiti et al., 2010). The two full-length *ZmHb1* and *ZmHb2* cDNAs were cloned into a pGEM-T Easy Vector System (Promega). The two cDNAs were subsequently amplified from the vector using T7 and SP6 primers and used for the preparation of digoxigenin-labeled sense and antisense riboprobes following the procedure outlined in the DIG Application Manual (Roche Diagnostics). Slide preparation, hybridization conditions, and color development were performed as documented previously (Elhiti et al., 2010).

Statistical Analysis

Tukey's post hoc test (Zar, 1999) was used for comparison and analysis of significant differences.

Supplemental Data

The following materials are available in the online version of this article.

Supplemental Figure S1. Amino acid sequence alignment of *ZmHb1* and *ZmHb2* with Clustal W using BLOSUM protein weight matrix (Larkin et al., 2007).

Supplemental Figure S2. Regulation of *ZmHb1* and *ZmHb2* by auxin.

Supplemental Figure S3. Detection of Zn^{2+} in maize embryos by Zinquin.

Supplemental Figure S4. Effects of increasing concentrations of the NO donor (DEA/NO) on the release of Zn^{2+} from a constant concentration of recombinant ZmMT4 protein (Table I).

Supplemental Figure S5. Percentage of TUNEL-positive cells in immature (d 7, P medium) embryos cultured in environments with altered levels of NO and Zn^{2+}.

Supplemental Figure S6. Cytological and molecular hallmarks of PCD in *ZmHb*-suppressing embryos.

Supplemental Figure S7. Localization of reduced ASC in immature (d 7, P medium) maize embryos produced by the wild-type line and *ZmHb1(A)* and *ZmHb2(A)* lines.

Supplemental Figure S8. Expression level of four respiratory burst oxidase homologs (*ZmrbohA-D*) in immature embryos (d 7, P medium) produced from the wild-type lines and *ZmHb1(A)* and *ZmHb2(A)* lines.

Supplemental Table S1. List of primers used in this study.

ACKNOWLEDGMENTS

We thank Doug Durnin for technical assistance.

Received March 10, 2014; accepted April 22, 2014; published May 1, 2014.

LITERATURE CITED

Aravindakumar CT, Ceulemans J, De Ley M (1999) Nitric oxide induces Zn^{2+} release from metallothionein by destroying zinc-sulphur clusters without concomitant formation of S-nitrosothiol. Biochem J **344:** 253–258

Bayraktutan U (2005) Coronary microvascular endothelial cell growth regulates expression of the gene encoding p22-phox. Free Radic Biol Med **39:** 1342–1352

Berendji D, Kolb-Bachofen V, Meyer KL, Grapenthin O, Weber H, Wahn V, Kröncke KD (1997) Nitric oxide mediates intracytoplasmic and intranuclear zinc release. FEBS Lett **405:** 37–41

Bindschedler LV, Dewdney J, Blee KA, Stone JM, Asai T, Plotnikov J, Denoux C, Hayes T, Gerrish C, Davies DR, et al (2006) Peroxidase-dependent apoplastic oxidative burst in Arabidopsis required for pathogen resistance. Plant J **47:** 851–863

Blanvillain R, Young B, Cai YM, Hecht V, Varoquaux F, Delorme V, Lancelin JM, Delseny M, Gallois P (2011) The Arabidopsis peptide kiss of death is an inducer of programmed cell death. EMBO J **30:** 1173–1183

Bosch M, Franklin-Tong VE (2007) Temporal and spatial activation of caspase-like enzymes induced by self-incompatibility in Papaver pollen. Proc Natl Acad Sci USA **104:** 18327–18332

Bozhkov PV, Filonova LH, Suarez MF (2005) Programmed cell death in plant embryogenesis. Curr Top Dev Biol **67:** 135–179

Bradford MM (1976) A rapid and sensitive method for the quantitation of microgram quantities of protein utilizing the principle of protein-dye binding. Anal Biochem **72:** 248–254

Brittain T, Skommer J, Raychaudhuri S, Birch N (2010) An antiapoptotic neuroprotective role for neuroglobin. Int J Mol Sci **11:** 2306–2321

Browning DD, McShane MP, Marty C, Ye RD (2000) Nitric oxide activation of p38 mitogen-activated protein kinase in 293T fibroblasts requires cGMP-dependent protein kinase. J Biol Chem **275:** 2811–2816

Brüne B (2003) Nitric oxide: NO apoptosis or turning it ON? Cell Death Differ **10:** 864–869

Burmester T, Hankeln T (2009) What is the function of neuroglobin? J Exp Biol **212:** 1423–1428

Cobbett CS, Goldsbrough PB (2002) Phytochelatins and metallothioneins: roles in heavy metal detoxification and homeostasis. Annu Rev Plant Biol **53:** 159–182

Coffeen WC, Wolpert TJ (2004) Purification and characterization of serine proteases that exhibit caspase-like activity and are associated with programmed cell death in Avena sativa. Plant Cell **16:** 857–873

Cuajungco MP, Lees GJ (1998) Nitric oxide generators produce accumulation of chelatable zinc in hippocampal neuronal perikarya. Brain Res **799:** 118–129

Davies DR, Bindschedler LV, Strickland TS, Bolwell GP (2006) Production of reactive oxygen species in *Arabidopsis thaliana* cell suspension cultures in response to an elicitor from *Fusarium oxysporum*: implications for basal resistance. J Exp Bot **57:** 1817–1827

Diatchuk V, Lotan O, Koshkin V, Wikstroem P, Pick E (1997) Inhibition of NADPH oxidase activation by 4-(2-aminoethyl)-benzenesulfonyl fluoride and related compounds. J Biol Chem **272:** 13292–13301

Dordas C, Hasinoff BB, Igamberdiev AU, Manac'h N, Rivoal J, Hill RD (2003) Expression of a stress-induced hemoglobin affects NO levels produced by alfalfa root cultures under hypoxic stress. Plant J **35:** 763–770

Drummond GR, Selemidis S, Griendling KK, Sobey CG (2011) Combating oxidative stress in vascular disease: NADPH oxidases as therapeutic targets. Nat Rev Drug Discov **10:** 453–471

Earley KW, Haag JR, Pontes O, Opper K, Juehne T, Song K, Pikaard CS (2006) Gateway-compatible vectors for plant functional genomics and proteomics. Plant J **45:** 616–629

Elhiti M, Hebelstrup KH, Wang A, Li C, Cui Y, Hill RD, Stasolla C (2013) Function of type-2 Arabidopsis hemoglobin in the auxin-mediated formation of embryogenic cells during morphogenesis. Plant J **74:** 946–958

Elhiti M, Tahir M, Gulden RH, Khamiss K, Stasolla C (2010) Modulation of embryo-forming capacity in culture through the expression of Brassica genes involved in the regulation of the shoot apical meristem. J Exp Bot **61:** 4069–4085

Elmore S (2007) Apoptosis: a review of programmed cell death. Toxicol Pathol **35:** 495–516

Evans DE (2003) Aerenchyma formation. New Phytol **161:** 35–49

Favata MF, Horiuchi KY, Manos EJ, Daulerio AJ, Stradley DA, Feeser WS, Van Dyk DE, Pitts WJ, Earl RA, Hobbs F, et al (1998) Identification of a novel inhibitor of mitogen-activated protein kinase kinase. J Biol Chem **273:** 18623–18632

Filonova LH, Bozhkov PV, Brukhin VB, Daniel G, Zhivotovsky B, von Arnold S (2000) Two waves of programmed cell death occur during formation and development of somatic embryos in the gymnosperm, Norway spruce. J Cell Sci **113:** 4399–4411

Garrocho-Villegas V, de Jesús-Olivera MT, Quintanar ES (2012) Maize somatic embryogenesis: recent features to improve plant regeneration. Methods Mol Biol **877:** 173–182

Greenberg DA, Jin K, Khan AA (2008) Neuroglobin: an endogenous neuroprotectant. Curr Opin Pharmacol **8:** 20–24

Hebelstrup KH, Jensen EO (2008) Expression of NO scavenging hemoglobin is involved in the timing of bolting in *Arabidopsis thaliana*. Planta **227:** 917–927

Hegelund JN, Schiller M, Kichey T, Hansen TH, Pedas P, Husted S, Schjoerring JK (2012) Barley metallothioneins: MT3 and MT4 are localized in the grain aleurone layer and show differential zinc binding. Plant Physiol **159:** 1125–1137

Helmersson A, von Arnold S, Bozhkov PV (2008) The level of free intracellular zinc mediates programmed cell death/cell survival decisions in plant embryos. Plant Physiol **147:** 1158–1167

Hill RD (2012) Non-symbiotic haemoglobins: What's happening beyond nitric oxide scavenging? AoB Plants **2012:** pls004

Hunt PW, Watts RA, Trevaskis B, Llewelyn DJ, Burnell J, Dennis ES, Peacock WJ (2001) Expression and evolution of functionally distinct haemoglobin genes in plants. Plant Mol Biol **47:** 677–692

Igamberdiev AU, Stasolla C, Hill RD (2014) Low oxygen stress, non-symbiotic hemoglobins, NO and programmed cell death. *In* **van Dongen JT, Licausi F**, eds, Oxygen Stress in Plants. Springer-Verlag, Berlin, pp 41–58

Igamberdiev AU, Stoimenova M, Seregélyes C, Hill RD (2006) Class-1 hemoglobin and antioxidant metabolism in alfalfa roots. Planta **223:** 1041–1046

Karimi M, Inzé D, Depicker A (2002) GATEWAY vectors for Agrobacterium-mediated plant transformation. Trends Plant Sci **7:** 193–195

Keshet Y, Seger R (2010) The MAP kinase signaling cascades: a system of hundreds of components regulates a diverse array of physiological functions. Methods Mol Biol **661:** 3–38

Khan AA, Mao XO, Banwait S, Jin K, Greenberg DA (2007) Neuroglobin attenuates beta-amyloid neurotoxicity in vitro and transgenic Alzheimer phenotype in vivo. Proc Natl Acad Sci USA **104:** 19114–19119

Land PW, Aizenman E (2005) Zinc accumulation after target loss: an early event in retrograde degeneration of thalamic neurons. Eur J Neurosci **21:** 647–657

Larkin MA, Blackshields G, Brown NP, Chenna R, McGettigan PA, McWilliam H, Valentin F, Wallace IM, Wilm A, Lopez R, et al (2007) Clustal W and Clustal X version 2.0. Bioinformatics **23:** 2947–2948

Lee JY, Kim JH, Palmiter RD, Koh JY (2003) Zinc released from metallothionein-III may contribute to hippocampal CA1 and thalamic neuronal death following acute brain injury. Exp Neurol **184:** 337–347

Lee SJ, Koh JY (2010) Roles of zinc and metallothionein-3 in oxidative stress-induced lysosomal dysfunction, cell death, and autophagy in neurons and astrocytes. Mol Brain **3:** 30

Leszczyszyn OI, Imam HT, Blindauer CA (2013) Diversity and distribution of plant metallothioneins: a review of structure, properties and functions. Metallomics **5:** 1146–1169

Lin F, Ding H, Wang J, Zhang H, Zhang A, Zhang Y, Tan M, Dong W, Jiang M (2009a) Positive feedback regulation of maize NADPH oxidase by mitogen-activated protein kinase cascade in abscisic acid signalling. J Exp Bot **60:** 3221–3238

Lin ZF, Liu N, Lin GZ, Peng CL (2009b) In situ localisation of superoxide generated in leaves of *Alocasia macrorrhiza* (L.) Shott under various stresses. J Plant Biol **52:** 340–347

Liso R, De Tullio MC, Ciraci S, Balestrini R, La Rocca N, Bruno L, Chiappetta A, Bitonti MB, Bonfante P, Arrigoni O (2004) Localization of ascorbic acid, ascorbic acid oxidase, and glutathione in roots of *Cucurbita maxima* L. J Exp Bot **55:** 2589–2597

Livak KJ, Schmittgen TD (2001) Analysis of relative gene expression data using real-time quantitative PCR and the 2(-Delta Delta C(T)) method. Methods **25:** 402–408

Miller MR, Megson IL (2007) Recent developments in nitric oxide donor drugs. Br J Pharmacol **151:** 305–321

Mur LA, Mandon J, Cristescu SM, Harren FJ, Prats E (2011) Methods of nitric oxide detection in plants: a commentary. Plant Sci **181:** 509–519

Mur LA, Sivakumaran A, Mandon J, Cristescu SM, Harren FJ, Hebelstrup KH (2012) Haemoglobin modulates salicylate and jasmonate/ethylene-mediated resistance mechanisms against pathogens. J Exp Bot **63:** 4375–4387

Paradkar RP, Williams RR (1994) Micellar colorimetric determination of dithizone metal chelates. Anal Chem **66:** 2752–2756

Pennell RI, Lamb C (1997) Programmed cell death in plants. Plant Cell **9:** 1157–1168

Portt L, Norman G, Clapp C, Greenwood M, Greenwood MT (2011) Anti-apoptosis and cell survival: a review. Biochim Biophys Acta **1813:** 238–259

Potters G, De Gara L, Asard H, Horemans N (2002) Ascorbate and glutathione: guardians of the cell cycle, partners in crime? Plant Physiol Biochem **40:** 537–548

Reape TJ, Molony EM, McCabe PF (2008) Programmed cell death in plants: distinguishing between different modes. J Exp Bot **59:** 435–444

Ren Y, Liu Y, Chen H, Li G, Zhang X, Zhao J (2012) Type 4 metallothionein genes are involved in regulating Zn ion accumulation in late embryo and in controlling early seedling growth in Arabidopsis. Plant Cell Environ **35:** 770–789

Rogers JM, Taubeneck MW, Daston GP, Sulik KK, Zucker RM, Elstein KH, Jankowski MA, Keen CL (1995) Zinc deficiency causes apoptosis but not cell cycle alterations in organogenesis-stage rat embryos: effect of varying duration of deficiency. Teratology **52:** 149–159

Roohani N, Hurrell R, Kelishadi R, Schulin R (2013) Zinc and its importance for human health: an integrative review. J Res Med Sci **18:** 144–157

Ryder LS, Dagdas YF, Mentlak TA, Kershaw MJ, Thornton CR, Schuster M, Chen J, Wang Z, Talbot NJ, Talbot NJ (2013) NADPH oxidases regulate septin-mediated cytoskeletal remodeling during plant infection by the rice blast fungus. Proc Natl Acad Sci USA **110:** 3179–3184

Sagi M, Fluhr R (2006) Production of reactive oxygen species by plant NADPH oxidases. Plant Physiol **141:** 336–340

Samuel MA, Ellis BE (2002) Double jeopardy: both overexpression and suppression of a redox-activated plant mitogen-activated protein kinase render tobacco plants ozone sensitive. Plant Cell **14:** 2059–2069

Schrantz N, Auffredou MT, Bourgeade MF, Besnault L, Leca G, Vazquez A (2001) Zinc-mediated regulation of caspases activity: dose-dependent inhibition or activation of caspase-3 in the human Burkitt lymphoma B cells (Ramos). Cell Death Differ **8:** 152–161

Smagghe BJ, Blervacq AS, Blassiau C, Decottignies JP, Jacquot JP, Hargrove MS, Hilbert JL (2007) Immunolocalization of non-symbiotic hemoglobins during somatic embryogenesis in chicory. Plant Signal Behav **2:** 43–49

Smagghe BJ, Hoy JA, Percifield R, Kundu S, Hargrove MS, Sarath G, Hilbert JL, Watts RA, Dennis ES, Peacock WJ, et al (2009) Review: correlations between oxygen affinity and sequence classifications of plant hemoglobins. Biopolymers **91:** 1083–1096

Smertenko A, Bozhkov PV (2014) Somatic embryogenesis: life and death processes during apical-basal patterning. J Exp Bot **65:** 1343–1360

Stasolla C, Yeung EC (1999) Ascorbic acid improves conversion of white spruce somatic embryos. In Vitro Cell Dev Biol Plant **35:** 316–319

St Croix CM, Wasserloos KJ, Dineley KE, Reynolds IJ, Levitan ES, Pitt BR (2002) Nitric oxide-induced changes in intracellular zinc homeostasis are mediated by metallothionein/thionein. Am J Physiol Lung Cell Mol Physiol **282:** L185–L192

Thordal-Christensen H, Zhang Z, Wei Y, Collinge DB (1997) Subcellular localization of H_2O_2 in plants. H_2O_2 accumulation in papillae and hypersensitive response during the barley-powdery mildew interaction. Plant J **11:** 1187–1194

Thorpe TA, Stasolla C (2001) Somatic embryogenesis. *In* Bhojwani SS, Soh WY, eds, Current Trends in the Embryology of Angiosperms. Kluwer Academic Publisher, Dordrecht, pp 279–336

Tiwari BS, Belenghi B, Levine A (2002) Oxidative stress increased respiration and generation of reactive oxygen species, resulting in ATP depletion, opening of mitochondrial permeability transition, and programmed cell death. Plant Physiol **128:** 1271–1281

Torres MA, Dangl JL (2005) Functions of the respiratory burst oxidase in biotic interactions, abiotic stress and development. Curr Opin Plant Biol **8:** 397–403

Truong-Tran AQ, Ho LH, Chai F, Zalewski PD (2000) Cellular zinc fluxes and the regulation of apoptosis/gene-directed cell death. J Nutr (5SSuppl) **130:** 1459S–1466S

Van Breusegem F, Dat JF (2006) Reactive oxygen species in plant cell death. Plant Physiol **141:** 384–390

van Doorn WG, Beers EP, Dangl JL, Franklin-Tong VE, Gallois P, Hara-Nishimura I, Jones AM, Kawai-Yamada M, Lam E, Mundy J, et al (2011) Morphological classification of plant cell deaths. Cell Death Differ **18:** 1241–1246

Vázquez-Limón C, Hoogewijs D, Vinogradov SN, Arredondo-Peter R (2012) The evolution of land plant hemoglobins. Plant Sci **191-192:** 71–81

Wang K, Frame B (2009) Biolistic gun-mediated maize genetic transformation. Methods Mol Biol **526:** 29–45

Wang PC, Du YY, Li Y, Ren DT, Song CP (2010) Hydrogen peroxide-mediated activation of MAP kinase 6 modulates nitric oxide biosynthesis and signal transduction in *Arabidopsis*. Plant Cell **22:** 2981–2998

Wätjen W, Cox M, Biagioli M, Beyersmann D (2002) Cadmium-induced apoptosis in C6 glioma cells: mediation by caspase 9-activation. Biometals **15:** 15–25

Weber RE, Vinogradov SN (2001) Nonvertebrate hemoglobins: functions and molecular adaptations. Physiol Rev **81:** 569–628

Whelan RS, Kaplinskiy V, Kitsis RN (2010) Cell death in the pathogenesis of heart disease: mechanisms and significance. Annu Rev Physiol **72:** 19–44

Wind S, Beuerlein K, Eucker T, Müller H, Scheurer P, Armitage ME, Ho H, Schmidt HH, Wingler K (2010) Comparative pharmacology of chemically distinct NADPH oxidase inhibitors. Br J Pharmacol **161:** 885–898

Ye Y, Li Z, Xing D (2013) Nitric oxide promotes MPK6-mediated caspase-3-like activation in cadmium-induced Arabidopsis thaliana programmed cell death. Plant Cell Environ **36:** 1–15

Zalewski PD, Forbes IJ, Betts WH (1993) Correlation of apoptosis with change in intracellular labile Zn(II) using zinquin [(2-methyl-8-p-toluenesulphonamido-6-quinolyloxy)acetic acid], a new specific fluorescent probe for Zn(II). Biochem J **296:** 403–408

Zar J (1999) Biostatistical Analysis, Ed 4. Prentice-Hall, Upper Saddle River NJ, pp 177–230

Zhang Y, Aizenman E, DeFranco DB, Rosenberg PA (2007) Intracellular zinc release, 12-lipoxygenase activation and MAPK dependent neuronal and oligodendroglial death. Mol Med **13:** 350–355

Zhao L, Gu RL, Gao P, Wang GY (2008) A nonsymbiotic hemoglobin gene from maize, ZmHb, is involved in response to submergence, high-salt and osmotic stresses. Plant Cell Tissue Organ Cult **95:** 227–237